

Envelope Simulation by SPICE-Compatible Models of Linear Electric Circuits Driven by Modulated Signals

Shmuel Ben-Yaakov, *Member, IEEE*, Stanislav Glazman, and Raul Rabinovici, *Senior Member, IEEE*

Abstract—SPICE-compatible equivalent circuits were developed to facilitate the analysis and envelope simulation of electric circuits driven by modulated signals. The circuits are based on a novel complex phasor-domain transformation. The proposed method facilitates simulation of any general linear circuit driven by a modulated signal such as amplitude modulation, frequency modulation, or phase modulation. Simulation time by the proposed envelope simulation is much faster than the full cycle-by-cycle simulation of the original circuit and excitation.

Index Terms—Amplitude modulation, computer-aided analysis, envelope detection, inverters, modeling, modulation, phase modulation, power system simulation, resonant power conversion, simulation, SPICE.

I. INTRODUCTION

MODULATED signals play an important role in power electronics. For example, frequency modulation (FM) or phase modulation (PM) is related to resonant power converters [1] and electronic ballasts of discharge lamps [2]. Furthermore, amplitude modulation (AM) plays an important role in determining the stability of high-frequency electronic ballasts for discharge lamps [3], [4]. In these systems, the lamp is driven by a high-frequency source in series with an inductor which controls the current (Fig. 1). Power level is normally regulated by shifting the frequency of the source and thereby increasing or decreasing the current. Hence, current level can be closely controlled by a feedback network connected to a controlled oscillator that feeds the power stage. It should be noted that when the FM signal passes through reactive elements it would be translated to an amplitude-modulated FM signal. Direct analysis of the response of such an electrical circuit to a modulated carrier is thus complex while cycle-by-cycle simulation of such a system is very lengthy due to the presence of the high-frequency component.

The method proposed in [5] is based on a phasor transformation by which the original circuit of the high-frequency modulated carrier is transformed into an equivalent circuit of the low-

Paper MSDAD-S 00–32, presented at the 2000 IEEE Applied Power Electronics Conference and Exposition, New Orleans, LA, February 6–10, and approved for publication in the IEEE TRANSACTIONS ON INDUSTRY APPLICATIONS by the Production and Application of Light Committee of the IEEE Industry Applications Society. Manuscript submitted for review December 10, 1999 and released for publication November 28, 2000.

The authors are with the Department of Electrical and Computer Engineering, Ben-Gurion University of the Negev, Beer-Sheva 84105, Israel (e-mail: sby@ee.bgu.ac.il).

Publisher Item Identifier S 0093-9994(01)02104-1.

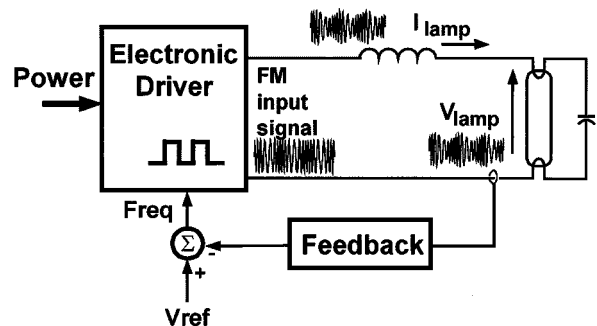


Fig. 1. Fluorescent lamp, driven by a high-frequency source in series with an inductor which controls the current.

frequency modulation signals. In this transformation, the resistance components are equivalent to themselves, but the equivalent circuits of the reactive components include the component itself plus an "imaginary" resistor element. This technique was applied in limited studies for specialized cases, e.g., when the carrier frequency equals the resonant frequency of the circuit under examination [3], [4]. Still lacking thus far is a method that would facilitate envelope simulation by SPICE-based general-purpose circuit simulator such as PSPICE (MicroSim Inc., Beaverton, OR USA).

In this study, we developed a complex phasor transformation approach that was then used to derive a SPICE-compatible model transparent to the high-frequency carrier. The proposed method facilitates envelope simulation of any linear electric circuits by any general-purpose simulator. This approach differs from earlier solutions to envelope simulation which rely on specialized computer programs [6].

II. COMPLEX PHASOR TRANSFORMATION APPROACH

Any analog modulated signal (AM, FM, or PM) can be described by the following general expression:

$$u(t) = U_1(t) \cdot \cos(\omega_c t) + U_2(t) \cdot \sin(\omega_c t) \quad (1)$$

where $U_1(t)$ and $U_2(t)$ are the modulation signals and ω_c is the angular frequency of the carrier.

Expression (1) could also be written as

$$u(t) = \text{Re}[(U_1(t) - j \cdot U_2(t)) \cdot \exp(j\omega_c t)] \quad (2)$$

or as

$$u(t) = |U(t)| \cdot \text{Re}[\exp(\arg(U(t))) \cdot \exp(j\omega_c t)] \quad (3)$$

where " $\arg(U(t))$ " is $\tan^{-1}(-U_2(t)/U_1(t))$.

Expression (3) implies that the modulated signal in the time domain $u(t)$ can be represented by a generalized phasor that both its magnitude and phase are time dependent. The expression of the complex phasor $\vec{U}(t)$ is

$$\vec{U}(t) = U_1(t) - jU_2(t). \quad (4)$$

The magnitude

$$|\vec{U}(t)| = [U_1^2(t) + U_2^2(t)]^{1/2} \quad (5)$$

is equal to the modulation envelope of the original signal $u(t)$ (3).

As will be shown next, the complex phasor representation $\vec{U}(t) = U_1(t) - jU_2(t)$, introduced here, can be used to drive the low-frequency equivalent circuits that represent the envelope behavior of the system without involving the high frequency carrier. This would shorten simulation time considerably since the time-domain analysis does not include the high-frequency component. The equivalent circuit is obtained similarly to [5] by a phasor transformation of the electric components L , C , and R . An inductor L in the original circuit becomes an inductive component L in series with an imaginary resistor $j\omega_c L$ in the equivalent circuit, a capacitive component C becomes a capacitor C in parallel to an imaginary resistor $1/(j\omega_c C)$, and a resistor component R is equivalent to the same resistor component R . Therefore, the equivalent circuit in the generalized phasor domain will consist of inductors, capacitors, and resistors in series or in parallel to "imaginary" resistors. Such a circuit is not compatible with SPICE simulators and, consequently, an additional transformation is needed to permit simulation by common circuit simulators. This additional step is described in the following section.

III. SPICE MODELS FOR CIRCUITS WITH IMAGINARY RESISTORS

The proposed methodology is demonstrated by considering an L , R circuit [Fig. 2(a)] driven by a generalized modulated signal

$$v(t) = V_1(t) \cos(\omega_c t) + V_2(t) \sin(\omega_c t). \quad (6)$$

The equivalent circuit in the generalized phasor domain [Fig. 2(b)] can be described by

$$\vec{V}(t) = R\vec{I}(t) + L\frac{d\vec{I}(t)}{dt} + j\omega_c L\vec{I}(t) \quad (7)$$

where the last term could be interpreted as an "imaginary" resistor of the "value" $j\omega_c L$. $\vec{V}(t)$ and $\vec{I}(t)$ are the complex phasors that prevail in the equivalent circuit of Fig. 2(b)

$$\vec{V}(t) = V_1(t) - jV_2(t) \quad (8)$$

$$\vec{I}(t) = I_1(t) + jI_2(t). \quad (9)$$

Applying (8) and (9), (7) can be rewritten as

$$V_1 - jV_2 = R(I_1 + jI_2) + L\frac{d(I_1 + jI_2)}{dt} + j\omega_c L(I_1 + jI_2). \quad (10)$$

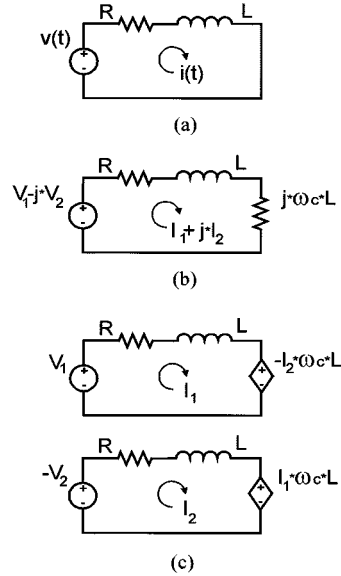


Fig. 2. SPICE model for a circuit with an "imaginary" resistor. (a) Original R , L circuit driven by a modulated voltage source. (b) Equivalent circuit of (a) in the generalized phasor domain. (c) Cross-coupled equivalent circuits based on (11) and (12) that replace (b).

To facilitate analysis by general-purpose circuit simulators, we divide the complex (10) into real and imaginary parts

$$V_1 = RI_1 + L\frac{dI_1}{dt} - \omega_c LI_2 \quad (\text{real}) \quad (11)$$

$$-V_2 = RI_2 + L\frac{dI_2}{dt} + \omega_c LI_1 \quad (\text{imaginary}). \quad (12)$$

The two equations, (11) and (12), can now be emulated by two interconnected circuits [Fig. 2(c)]. Notice that this representation does not involve imaginary resistors and that last terms in (11) and (12) are emulated by cross-coupled dependent voltage sources (a voltage source whose magnitude is a linear function of the current in the cross circuit). The newly developed equivalent circuits of Fig. 2(c) contain only conventional electric components and are, therefore, SPICE compatible. A similar but dual thinking can be followed for a capacitor in parallel with the "imaginary" resistor. For example, the equations for a capacitor C in parallel to a conductance G , fed by a current-source modulated signal, will be

$$I_1 = GV_1 + C\frac{dV_1}{dt} - \omega_c CV_2 \quad (\text{real}) \quad (13)$$

$$-I_2 = GV_2 + C\frac{dV_2}{dt} + \omega_c CV_1 \quad (\text{imaginary}). \quad (14)$$

Following this approach, SPICE-compatible circuits could be developed for more involved circuit configurations.

The usefulness of the proposed simulation method is further demonstrated by considering the case of a phase-modulated voltage source driving the circuit of Fig. 2(a). The source is assumed to be of the form

$$v(t) = A \cos[\omega_c t + m_p \sin(\omega_m t)]. \quad (15)$$

Therefore, the equivalent circuit of Fig. 2(b) is driven by the generalized voltage phasor

$$\vec{V}(t) = A \cos[m_p \sin(\omega_m t)] + jA \sin[m_p \sin(\omega_m t)]. \quad (16)$$

Consequently, the SPICE-compatible equivalent circuits of Fig. 2(c) are driven by the sources

$$V_1 = A \cos[m_p \sin(\omega_m t)] \quad (17)$$

$$-V_2 = A \sin[m_p \sin(\omega_m t)]. \quad (18)$$

The circuits of Fig. 2(c) were fed to a PSPICE simulator (evaluation version 8) via the Schematics Capture front end by using the appropriate symbols (dependent voltage sources are represented by EVALUATE symbols). The simulation was run for the following values: $R = 10 \Omega$, $L = 7 \text{ mH}$, $A = 200 \text{ V}$, $f_c = \omega_c/2\pi = 40 \text{ kHz}$, $m_p = 10$, $f_m = \omega_m/2\pi = 2 \text{ kHz}$.

Fig. 3(a) shows the original current i through the circuit of Fig. 2 (upper trace) and the envelope of the current, obtained by the circuits of Fig. 2(c) and applying (5) (lower trace). Fig. 3(b) compares the results of cycle-by-cycle simulation and envelope simulation. Fig. 3(c) depicts the voltage phasor components V_1 and $-V_2$, while Fig. 3(d) depicts the current phasor components I_1 and I_2 . The spectrum of the current of the original circuit [Fig. 2(a)] is shown in Fig. 4(a), while the spectrum of the reconstructed current is given in Fig. 4(b). The reconstruction was calculated by

$$i(t) = I_1(t) \cos(\omega_c t) + I_2(t) \sin(\omega_c t) \quad (19)$$

applying the original carrier frequency and the envelope component (I_1, I_2) of the SPICE simulation results based on Fig. 3(c). It is evident that both the envelope signals (Fig. 3) and the spectra (Fig. 4) obtained by the proposed simulation method are identical to the original ones.

IV. GENERAL CASE

Consider a general R, L, C circuit that is driven by a modulated carrier $u(t)$. The matrix state-space equation of the system is

$$\dot{x} = A \cdot x + B \cdot u. \quad (20)$$

By expressing u as the complex excitation (4), inserting it in (20) and breaking the resulting complex state-space equation into real and imaginary parts, one obtains

$$\dot{X}_1 = A \cdot X_1 - A_1 \cdot X_2 + B \cdot U_1 \quad (21)$$

$$\dot{X}_2 = A \cdot X_2 + A_1 \cdot X_1 - B \cdot U_2 \quad (22)$$

where X_1 and X_2 are the complex state variables of the phasor domain circuit, U_1 and U_2 are the source complex phasors, and A_1 is the matrix of the imaginary resistors, $j\omega_c L$ associated with each inductor and $1/j\omega_c C$ associated with each capacitor (ω_c is the carrier frequency). The cross-coupled terms $A_1 X_2$ in (21) and $A_1 X_1$ in (22) can be represented as dependent sources: voltage source in the inductor case and current source for the capacitor case. Original resistors are left as is. Equations (21) and (22) can now be simulated as two circuits that include dependent sources that are a function of the state variables of the cross circuits. Note that (21) and (22) include only the low-frequency component while the high-frequency carrier is present only as an algebraic coefficient (ω_c).

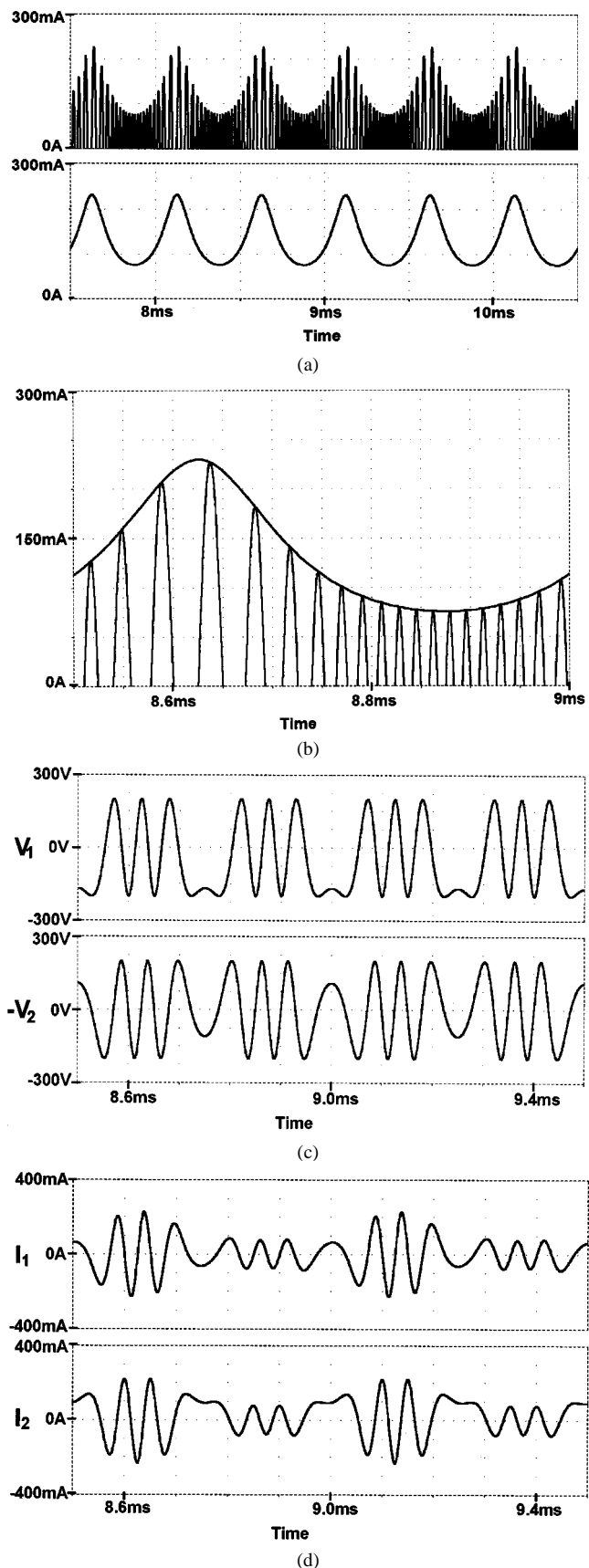


Fig. 3. Simulation results on the circuit of Fig. 2. (a) Current i through the original circuit of Fig. 2(a) (upper trace) and envelope of the current, obtained by envelope simulation based on Fig. 2(c) (lower trace). (b) Traces in (a) zoomed and superimposed. (c) Voltage phasor components V_1 and $-V_2$. (d) Current phasor components I_1 and I_2 .

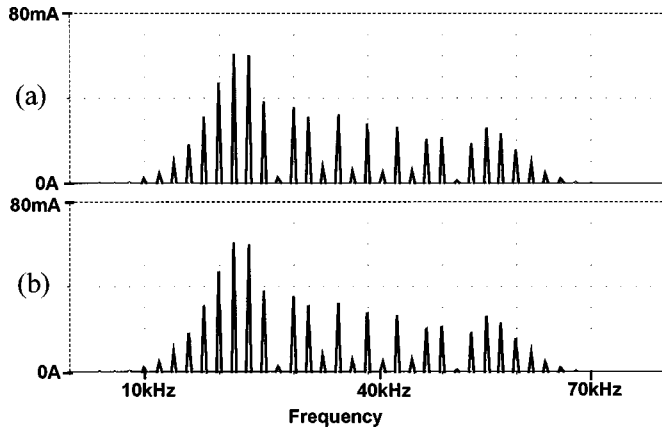


Fig. 4. Signal spectra. (a) Current in the original circuit [Fig. 2(a)]. (b) Reconstructed current spectrum. See text for details.

V. IMPLEMENTATION

Preparation of (21) and (22) for analysis by general-purpose analog circuit simulator can proceed by translating the equations into equivalent circuits. Matrix “ A ” is that of the original circuit, whereas “ A_1 ” is a new matrix representing the coupled dependent sources. Here, we describe a direct method that bypasses the need for constructing the new matrix. Starting with a general R, L, C circuit [Fig. 5(a)] that is driven by a modulated carrier $v(t)$, we first replace the reactive elements by dependent sources. An inductor L_i is replaced by a current source i_{L_i} and a capacitor C_i is replaced by a voltage source v_{C_i} [Fig. 5(b)]. The magnitude of the dependent sources is linked to auxiliary circuits that emulate the behavior of the elements. That is, the auxiliary circuit for L_i comprises a dependent voltage source v_{L_i} that forces the in-circuit voltage on the inductor L_i . The current generated in the auxiliary circuit is then fed back to the main circuit by the dependent current source i_{L_i} that represents the inductor. In a similar way, dependent voltage sources v_{C_i} replace capacitors in the main circuit. This separation step is not crucial but is used to streamline the structure of the equivalent circuits that will later evolve and allow automatization of the process.

The next step applies the transformation of the circuit into two phasor circuits per (21) and (22). Now, we apply the two phasor sources V_1 and $-V_2$ (as shown in Section III) and implement the dependent sources $A_1 X_2$ and $A_1 X_1$. These are shown schematically in Fig. 5(c) (real part) and Fig. 5(d) (imaginary part) for a specific inductor L_i and a capacitor C_i .

The state equations that represent an original inductor L_i [Fig. 5(a)] are, thus, for the real part [Fig. 5(c)]

$$L_i \cdot \frac{dI_{1L_i}}{dt} = V_{1L_i} + I_{2L_i} \cdot \omega_c \cdot L_i \quad (23)$$

and for the imaginary part [Fig. 5(d)]

$$L_i \cdot \frac{dI_{2L_i}}{dt} = V_{2L_i} - I_{1L_i} \cdot \omega_c \cdot L_i. \quad (24)$$

The state equations that represent an original capacitor C_i [Fig. 5(a)] are for the real part [Fig. 5(c)]

$$C_i \cdot \frac{dV_{1C_i}}{dt} = I_{1C_i} + V_{2C_i} \cdot \omega_c \cdot C_i \quad (25)$$

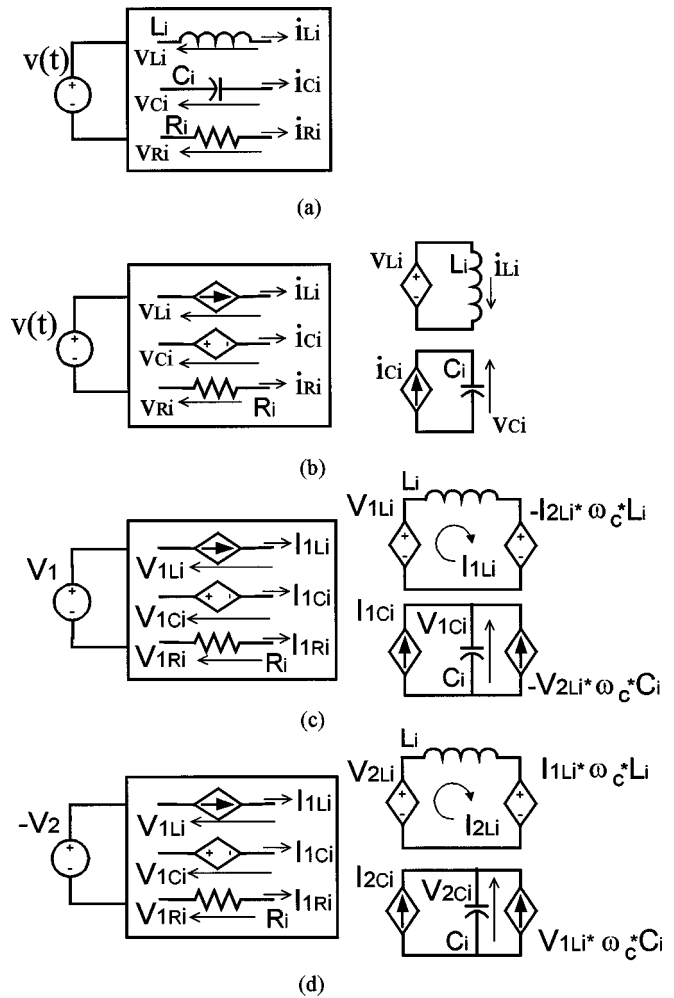


Fig. 5. Derivation of phasor equivalent circuits. (a) Original circuit. (b) Replacing reactive elements by dependent sources. (c) Real part of phasor equivalent circuit. (d) Imaginary part of phasor equivalent circuit.

and for the imaginary part [Fig. 5(d)]

$$C_i \cdot \frac{dV_{2C_i}}{dt} = I_{2C_i} - V_{1C_i} \cdot \omega_c \cdot C_i. \quad (26)$$

The equivalent circuits of Fig. 5(c) and (d) are now SPICE compatible. They include the original R, L, C components and dependent sources. It should be noted that the dependent sources are a function of the signals in the cross circuits. That is, the dependent sources in the real section [$-I_{2L_i} \cdot \omega_c \cdot L_i$, $-V_{2C_i} \cdot \omega_c \cdot C_i$, Fig. 5(c)] depend on the corresponding signals in the imaginary part [Fig. 5(d)] and vice versa.

The circuits of Fig. 5(c) and (d) are compatible with any modern circuit simulator. In the followings we present an example that was run on PSPICE (MicroSim Inc., Beaverton, OR USA, evaluation version 8), but any other simulator will do.

VI. EXAMPLE

We demonstrate the technique outlined above by considering a resonant circuit (Fig. 6). It is assumed that the circuit is driven by PM-modulated carrier of the form given above (15). The circuit was transformed according to the guidelines given above and the equivalent circuits (a total of six independent circuits)

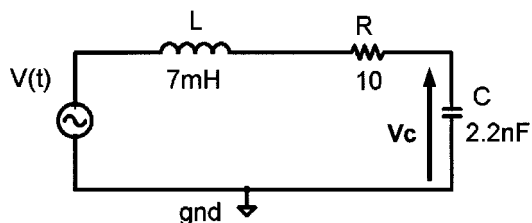


Fig. 6. Illustrative circuit.

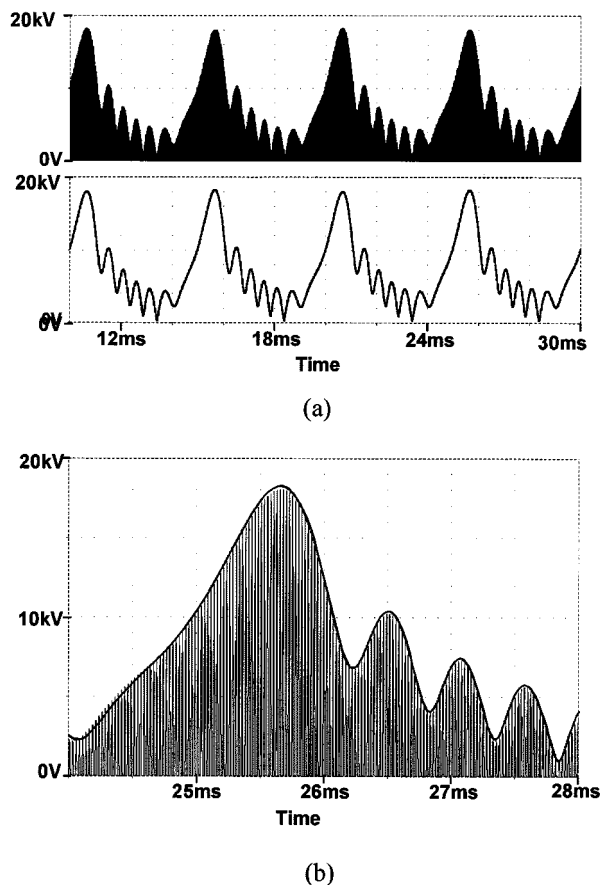


Fig. 7. Simulation results. (a) Real component of capacitor voltage (Fig. 6) (upper trace) and envelope as obtained by envelope simulation (lower trace). (b) Zoomed portion of (a).

were run on PSPICE. The phasor-domain sources are (17) and (18). For the purpose of illustration, we chose the carrier frequency ($f_c = \omega_c/2\pi$) to be 40.55 kHz equal to the circuit resonant frequency $1/2\pi\sqrt{LC}$. In the first run to be illustrated, the modulation parameters were: $A = 200$ V, $f_m = \omega_m/2\pi = 100$ Hz and $m_p = 20$. See the Appendix for netlist of the illustrative circuit.

Once the time-domain simulation is done, any of the envelope signals can be displayed. For example, the envelope of the capacitor voltage (V_C) is reconstructed by the expression

$$V_C = \sqrt{(V_{1C})^2 + (V_{2C})^2} \quad (27)$$

where V_{1C} and V_{2C} are the envelope simulation results obtained for the real and imaginary parts, respectively. The de-

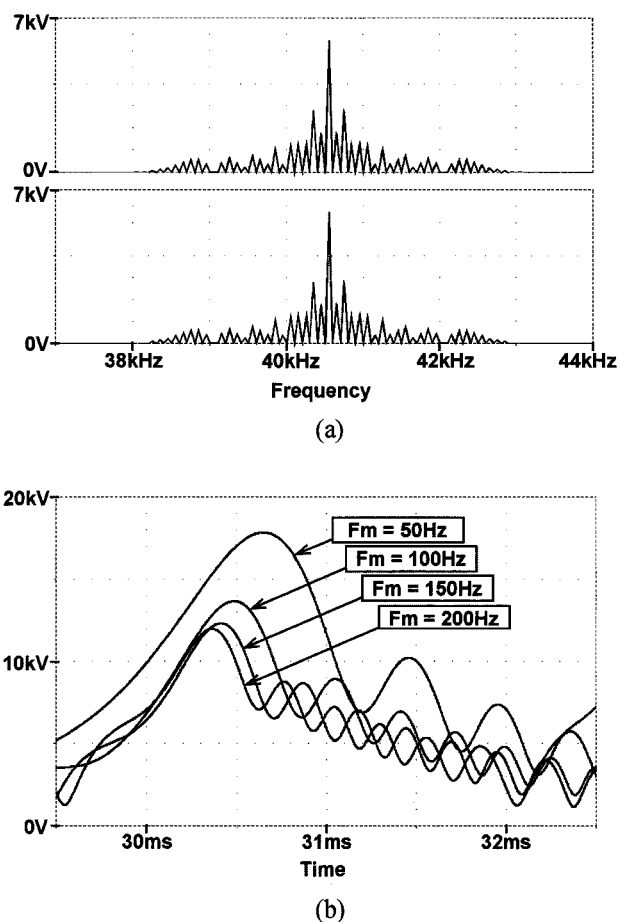


Fig. 8. Simulation results. (a) Spectrum of original circuit (upper trace) and reconstructed from envelope simulation (lower trace). (b) Envelope simulation of capacitor voltage (Fig. 6) for various modulating signals.

gree of matching between the real signal and the results of envelope simulation [Fig. 7(a)] demonstrate the agreement that is obtained. The perfect match is illustrated in the zoomed portion [Fig. 7(b)]. Furthermore, the original spectrum of the signal and the one reconstructed from the envelope simulation results are identical [Fig. 8(a)]. The simulation time for envelope simulation was 0.5 s as compared to 300 s with full simulation on circuit and modulated carrier. The CPU used was a 333-MHz Pentium.

Envelope simulation offers large flexibility and access to a wealth of information in a short simulation time. For example, the effect of the sweep speed on the capacitor voltage was explored by parametric simulation in which the modulating frequency was stepped from 50 to 200 Hz in 50-Hz steps while keeping the depth of modulation $m_p \cdot f_m = 4000$ constant [Fig. 8(b)]. Simulation time for this run was 10 s (on the same PC).

VII. DISCUSSION AND CONCLUSIONS

The general and systematic approach developed here offers a simple and straightforward procedure for generating SPICE-compatible phasor equivalent circuits of any R, L, C circuit driven by any modulated signal. The proposed equiv-

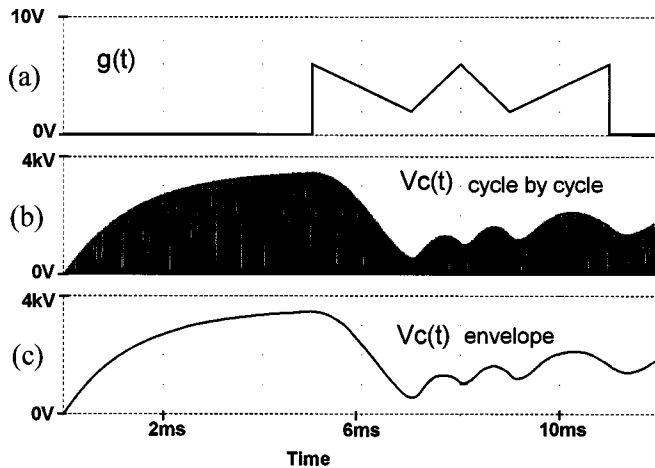


Fig. 9. Simulation results. (a) Arbitrary modulation function. (b) Capacitor voltage (Fig. 6) obtained by cycle-by-cycle simulation. (c) Capacitor voltage (Fig. 6) obtained by proposed envelope simulation.

alent circuits that were obtained by introducing the complex phasor representation are SPICE compatible and can, thus, be run on any general-purpose circuit simulator. Since envelope simulation involves only the low-frequency components, simulation time will be much shorter than the full-signal simulation. The time speedup will depend on the complexity of the circuit. For the simulation shown here, a speed up factor of about 1000:1 was observed. Although illustrated for the PM modulation case, FM and AM can be easily implemented as well. The FM case can be considered as a scaled case of PM, while the AM case is a truncated $v(t)$ signal including only a real part $V_1 = V_m \cdot [1 + m \cdot \cos(\omega_m t)]$. Note, however, that even in this case the imaginary equivalent circuit is still needed, but with $V_2 = 0$. It should be noted that the proposed simulation approach is not limited to sinusoidal modulation.

The proposed method is applicable to any modulation function $g(t)$. To illustrate this, we run a simulation on the same resonant circuit (Fig. 6), but with an arbitrary modulation function [Fig. 9(a)]. Matching between cycle-by-cycle simulation [Fig. 9(b)] and envelope simulation [Fig. 9(c)] was again excellent. The speedup factor was similar to the other cases (about 1000:1).

The systematic method for generating the auxiliary circuit is based on simple rules that can be easily mechanized to fully automate the transformation.

It can, thus, be concluded that the proposed envelope simulation is very efficient in terms of computer time. It should be noted that the method, as presented here, is applicable only to linear circuits.

APPENDIX

Given below are the netlist, definition of parameters, and Analysis Setup used in the simulations that generated the plots of this paper. The netlist is compatible with PSPICE Version 8. It would run on the evaluation (Demo) version. The netlist includes both the original *RLC* network and the subcircuits

of its envelope simulation model. If run together, the original circuit slows the simulation time.

The corresponding .sch file can be unloaded from: http://www.ee.bgu.ac.il/~pel/Envelope_Simulation/RLC.htm

```
* Envelope.sch
* Schematics Version 8.0 - July 1997
*Parameters of original RLC circuit
*(Rl is placed in series with inductors in en-
velope simulation subcircuits)
.PARAM L=7m Rl=1u
.PARAM C=2.2n R=100 Rc=1e10
*Parameters of FM modulated signal
.PARAM Km=100 Am=200
.PARAM Fm=100 Fc=40.1k
** Analysis setup **
.tran 20ns 15m 0 0.1u
*Schematics Netlist *
*Original RLC network
R_R r c {R}
C_C c 0 {C}
L_L in r {L} IC=0
E_Ein in 0 VALUE {
{Am}*cos(6.2832*{Fc}*time+{Km}*cos(6.2832*
+{Fm}*time)) }
*Envelope simulation subcircuits
*Definition of components: X_re=real part;
X_im=imaginary part;
EVL_re L_re 0 VALUE { V(in_re)-V(r_re) }
EVL_im L_im 0 VALUE { V(in_im)-V(r_im) }
Rl_re 2 1 {Rl}
Rl_im 4 3 {Rl}
L_re L_re 2 {L}
L_im L_im 4 {L}
R_re r_re cre {R}
R_im r_im cim {R}
Rc_re 0 C_re {Rc}
Rc_im 0 C_im {Rc}
C_re C_re 0 {C}
C_im C_im 0 {C}
GIC_re 0 C_re VALUE {-I(E_EC_re) }
GIC_im 0 C_im VALUE {-I(E_EC_im) }
GXC_re 0 C_re VALUE {-{Fc}*{C}*6.2832*V(C_im)}
GXC_im 0 C_im VALUE {{Fc}*{C}*6.2832*V(C_re)}
EXL_re 1 0 VALUE {
-{Fc}*6.2832*{L}*I(E_EVL_im) }
EXL_im 3 0 VALUE {{Fc}*6.2832*{L}*I(E_EVL_re)}
EC_re cre 0 VALUE { -V(C_re) }
EC_im cim 0 VALUE { -V(C_im) }
Ein_re in_re 0 VALUE {
{Am}*cos({Km}*cos(6.2832*{Fm}*time)) }
GL_im in_im r_im VALUE { -I(E_EVL_im) }
GL_re in_re r_re VALUE { -I(E_EVL_re) }
Ein_im in_im 0 VALUE {
-{Am}*sin({Km}*cos(6.2832* {Fm}*time)) }
.probe
.END
```

REFERENCES

- [1] R. L. Steigerwald, "High-frequency resonant transistor DC-DC converters," *IEEE Trans. Ind. Electron.*, vol. IE-31, pp. 182–190, May 1984.
- [2] B. C. Pollard and R. M. Nelms, "Using the series parallel resonant converter in capacitor charging applications," in *Proc. IEEE APEC'92*, 1992, pp. 731–37.
- [3] E. Deng, "I. Negative incremental impedance of fluorescent lamp," Ph.D. dissertation, Dept. Elect. Eng., California Inst. Technol., Pasadena, 1995.
- [4] E. Deng and S. Cuk, "Negative incremental impedance and stability of fluorescent lamp," in *Proc. IEEE APEC'97*, 1997, pp. 1050–1056.
- [5] C. T. Rim and G. H. Cho, "Phasor transformation and its application to the DC/AC analyzes of frequency phase-controlled series resonant converters (SRC)," *IEEE Trans. Power Electron.*, vol. 5, pp. 201–211, Apr. 1990.
- [6] D. Sharrit, "New method of analysis of communication systems," in *Proc. IEEE MIT Symp. WMFA: Nonlinear CAD Workshop*, June 1996.



Shmuel (Sam) Ben-Yaakov (M'87) was born in Tel Aviv, Israel, in 1939. He received the B.Sc. degree in electrical engineering from the Technion, Haifa, Israel, and the M.S. and Ph.D. degrees in engineering from the University of California, Los Angeles, in 1961, 1967, and 1970, respectively.

He is currently a Professor in the Department of Electrical and Computer Engineering, Ben-Gurion University of the Negev, Beer-Sheva, Israel, where he served as Chairman during the period 1985–1989.

He is also currently the Head of the Power Elec-

tronics Group. His current research interests include power electronics, circuits and systems, electronic instrumentation, and engineering education. He also serves as a Consultant to commercial companies on various subjects, including analog circuit design, modeling and simulation, PWM and resonant converters and inverters, soft-switching techniques, and electronic ballasts for discharge lamps.



Stanislav (Stas) Glozman was born in Tashkent, Uzbekistan, in 1972. He received the B.Sc. degree in electrical engineering in 1997 from Ben-Gurion University of the Negev, Beer-Sheva, Israel, where he is currently working toward the M.S. degree in electrical and computer engineering.

He is also currently involved in a research program in the Power Electronics Group at Ben-Gurion University of the Negev. His fields of interest include fluorescent lamp modeling and electronic ballast design.



Raul Rabinovici (M'83–SM'97) was born in Romania in 1950. He graduated as an electrical engineer from The Polytechnic Institute of Jassy, Jassy, Romania, and received the Ph.D. degree in electrical engineering from Ben-Gurion University of The Negev, Beer-Sheva, Israel, in 1972 and 1987, respectively.

He is currently a Senior Lecturer in the Department of Electrical and Computer Engineering, Ben-Gurion University of The Negev. Over the past eight years, his principal field of interest has been electric drives, including electric machines, power electronic drivers, DSP operation, and control algorithms. He is Co-Chairman of the International Steering Committee of the OPTIM Conference, Brasov, Romania.

Dr. Rabinovici was a member of the Editorial Board of the IEEE TRANSACTIONS ON MAGNETICS between 1996–1998.